Biochimica et Biophysica Acta 1788 (2009) 945–953

Contents lists available at ScienceDirect

Biochimica et Biophysica Acta

journal homepage: www.elsevier.com/locate/bbamem

Membrane hydration correlates to cellular biophysics during freezing in mammalian cells

Saravana K. Balasubramanian [a], Willem F. Wolkers [a], John C. Bischof [a,b,c,*]

[a] Department of Mechanical Engineering, University of Minnesota, 111 Church Street SE, Minneapolis, MN 55455, USA
[b] Biomedical Engineering, University of Minnesota, Minneapolis, MN 55455, USA
[c] Urologic Surgery, University of Minnesota, Minneapolis, MN 55455, USA

ARTICLE INFO

Article history:
Received 1 August 2008
Received in revised form 29 January 2009
Accepted 3 February 2009
Available online 21 February 2009

Keywords:
Cryosurgery
Cryopreservation
FTIR
Cryomicroscopy
Membrane phase behavior

ABSTRACT

Cell survival during freezing applications in biomedicine is highly correlated to the temperature history and its dependent cellular biophysical events of dehydration and intracellular ice formation (IIF). Although cell membranes are known to play a significant role in cell injury, a clear correlation between the membrane state and the surrounding intracellular and extracellular water is still lacking. We previously showed that lipid hydration in LNCaP tumor cells is related to cellular dehydration. The goal of this study is to build upon this work by correlating both the phase state of the membrane and the surrounding water to cellular biophysical events in three different mammalian cell types: human prostate tumor cells (LNCaP), human dermal fibroblasts (HDF), and porcine smooth muscle cells (SMC) using Fourier Transform Infrared spectroscopy (FTIR). Variable cooling rates were achieved by controlling the degree of supercooling prior to ice nucleation (−3 °C and −10 °C) while the sample was cooled at a set rate of 2 °C/min. Membranes displayed a highly cooperative phase transition under dehydrating conditions (i.e. NT = −3 °C), which was not observed under IIF conditions (NT = −10 °C). Spectral analysis showed a consistently greater amount of ice formation during dehydrating vs. IIF conditions in all cell types. This is hypothesized to be due to the extreme loss of membrane hydration in dehydrating cells that is manifested as excess water available for phase change. Interestingly, changes in residual membrane conformational disorder correlate strongly with cellular volumetric decreases as assessed by cryomicroscopy. A strong correlation was also found between the activation energies for freezing induced lyotropic membrane phase change determined using FTIR and the water transport measured by cryomicroscopy. Reduced lipid hydration under dehydration freezing conditions is suggested as one of the likely causes of what has been termed as "solution effects" injury in cryobiology.

1. Introduction

Cryogenic temperatures are used to preserve cells and tissues during cryopreservation, vitrification and freeze-drying, and to destroy cells in cryosurgery. The success of these applications depends on understanding the damaging effects of freezing at both the cellular and membrane level. At the cellular level, seminal work suggests a two factor hypothesis of freeze injury — "solution effects" injury due to exposure to increasing solute concentrations during slow freezing, and intracellular ice formation (IIF) due to cytoplasmic supercooling and consequent ice nucleation during rapid freezing [1]. At the membrane level, although model [2] and protoplast membrane dehydration and phase change have been measured and predicted during freezing [3,4], the link to cellular biophysics and injury is still not clear.

The mechanism of cell injury and subsequent death is an active area of research in the field of cryobiology. One of the primary sites for thermal injury is attributed to cell membranes [3,5,6]. Membrane damage resulting from high solute concentration [7], structural changes [8], and/or mechanical stress [9], have generally been implied in cell death during freeze induced dehydration. The membrane is in dynamic equilibrium with its surroundings and freezing affects the physical states of membrane lipids due to changes in hydration level (lyotropism) and temperature (thermotropism) [10]. The reorganization of lipids and changes in its residual membrane conformational disorder due to phase transitions from liquid crystalline to gel phase [4,11,12] or from liquid crystalline to hexagonal phase [3] under different thermal and hydration conditions have been implicated in injury. The consequences of these phase changes are thought to include increased membrane permeability and lateral phase separation of membrane components. In addition, exposure to reactive oxygen species could result in lipid peroxidation and phospholipid de-esterification [13]. Alterations in the lipid composition of the plasma membrane have also been causally related to cold acclimation of plant protoplasts [3].

* Corresponding author. Department of Mechanical Engineering, University of Minnesota, 111 Church Street SE, Minneapolis, MN 55455, USA. Tel.: +1 612 625 5513; fax: +1 612 625 4344.
E-mail address: bischof@umn.edu (J.C. Bischof).

0005-2736/$ – see front matter © 2009 Elsevier B.V. All rights reserved.
doi:10.1016/j.bbamem.2009.02.009

Cellular level freezing biophysics has been characterized by a number of techniques including cryomicroscopy and Differential Scanning Calorimetry (DSC). Cryomicroscopy measurements involve recording overall volumetric dehydration (by projected area measurements) or IIF (primarily by opacity changes i.e. "darkening") in cells during freezing [14,15]. The experimental data is then fit by mathematical models that allow prediction of dehydration and IIF kinetics for different freezing protocols [16–18]. Unfortunately, the cryomicroscopy technique cannot be extended to small or non-spherical cells and more complex biological systems, including tissues and organs. DSC is an alternative technique for quantifying dehydration kinetics in cells and tissues [19–21]. The measurement is indirect in that it relies on quantifying excess heat release during conditions that favor cellular dehydration (i.e. availability of excess water) that is unavailable during IIF or cell lysis. While cryomicroscopy and DSC are powerful tools, they do not provide insights into the underlying macromolecular mechanisms of freeze injury. Hence, techniques that quantify cellular freezing biophysics and the associated injury at the molecular level, independent of cell shape, are needed.

Fourier Transform Infra-Red (FTIR) spectroscopy is increasingly being applied to study cells in a variety of physical sample states, including hydrated, frozen, and dried. FTIR can be used to quantify thermotropic and lyotropic membrane phase changes in cells and tissues [22]. Previously, we have characterized and related the effect of ice nucleation temperature during slow cooling on the lyotropic response of human LNCaP prostate tumor cell membranes to cell viability [12]. The highest cell viability was observed under freezing conditions with intermediate dehydration and IIF [12]. Under conditions that cause cellular dehydration, membranes display a highly cooperative phase transition resulting in a strongly packed gel phase in the frozen state. This indicates that reduced lipid hydration may play a role in determining viability outcome [12]. Membrane lipid phase changes in cellular systems are monitored using the symmetric $-CH_2$ stretching vibration [23,24]. In addition, the state of water during freezing can be interrogated using the libration and bending combination vibration mode of H_2O.

In spite of tremendous progress in the field, the behavior of cell membranes during freezing and how their response correlates to cellular biophysical events have not yet been clearly established. The goal of the present study is to build upon our previous results [12] to correlate cellular biophysical events, during slow freezing (dehydrating conditions) and uncontrolled fast freezing (IIF conditions), to the state of water and the cell membrane. The phase state of the membrane is used here to refer to the state of the membrane lipids at a particular temperature as a consequence of the imposed freezing constraints. Using FTIR, membrane and water spectra were investigated during controlled freezing in three different cell types: human dermal fibroblasts (HDF), porcine smooth muscle cells (SMC) and human LNCaP prostate tumor cells (from [12]). The results show: (1) a unique membrane phase change for each cell that correlates to injurious cellular biophysical events, and (2) a consistently greater amount of ice formed during dehydrating vs. IIF conditions in all cells.

2. Materials and methods

2.1. Cell culture

2.1.1. Human dermal fibroblasts (HDF)

Neonatal HDF were obtained from cryopreserved stock (Cambrex, East Rutherford, NJ) and cultured in Dulbecco's modified Eagle medium (DMEM) containing 10% fetal bovine serum (FBS) and 1% penicillin/streptomycin (p/s) in saline (Invitrogen, Carlsbad, CA).

2.1.2. LNCaP Pro 5 tumor cells

LNCaP were obtained from cryopreserved stock (MD Anderson Cancer Center, Houston, TX) and cultured in DMEM F-12 media Invitrogen, Carsbad, CA supplemented with 10% FBS and 1% p/s in saline.

2.1.3. Porcine smooth muscle cells (SMC)

SMCs were isolated from explanted porcine femoral arteries as described previously [25]. Briefly, the arteries were cut into small pieces and placed in Petri dishes allowing cells to grow out of the tissues [26]. SMC media was composed of DMEM F-12 (Invitrogen, Carsbad, CA) containing 10% FBS, 1% p/s in saline and 1% L-glutamine. All SMC cells used for experiments were from passage 4 of culture.

2.1.4. Cell harvesting

Cells were cultured in T-75 flasks for 3–4 days up to 80% confluency. All cells were then trypsinized using 0.05% Trypsin with 0.53 mM EDTA (Invitrogen, Carslbad, CA). The trypsin was inactivated using serum filled media. Cells were then centrifuged at 400 g for 10 min, the media removed and 12 μL of the cell pellet was sandwiched between CaF_2 windows for FTIR analysis.

2.2. Cellular biophysical model

The phenomenological mathematical model used to predict cellular dehydration was first developed for cells in suspension [17]. Briefly, during freezing, the osmotic balance across the cell membrane is affected by the solute concentration in the extracellular space. Eq. (1) models the water movement across the cell membrane to achieve chemical equilibrium.

$$\frac{dV}{dT} = \frac{L_p ART}{Bv_w}\left[\ln\frac{(V - V_b)}{(V - V_b) + v_w v_s n_s} - \frac{\Delta H_f}{R}\left(\frac{1}{T_{ref}} - \frac{1}{T}\right)\right]. \quad (1)$$

In the above equation, V is the volume of the cell (μm^3); T is the absolute temperature (K); T_{ref} is the reference temperature (273.15 K); A is the surface area of the cell (μm^2); R is the universal gas constant (8.314 J/mol.K); v_w is the molar volume of water (μm^3/mol); v_s is the disassociation coefficient of salt (2); n_s is the number of moles of salt in the cell (mol); L_p is the hydraulic permeability of the cell (μm^3/N s); V_b is the osmotically inactive volume of the cell (μm^3); ΔH_f is the latent heat of fusion for water (kJ/mol); and B is the cooling rate (°C/min). Variation in the cell membrane hydraulic permeability (L_p) is modeled using an Arrhenius relationship [16] (Eq. (2)).

$$L_p = L_{pg}\exp\left[\frac{-E_{Lp}}{R}\left(\frac{1}{T} - \frac{1}{T_{ref}}\right)\right]. \quad (2)$$

Here, L_{pg} is the membrane hydraulic permeability at T_{ref} (μm/min atm) and E_{Lp} is the activation energy for water transport (kcal/mol). A detailed discussion of the assumptions made in the above equations has been given elsewhere [1,27,28].

In order to use this model for comparison to FTIR data in the present study (see Fig. 6), parameters from previous cryomicroscopy experiments were used. These included the initial and non-solvent volumes ($V_o = 716$, 1806, 932 μm^3; $V_b/V_o = 0.24$, 0.07, 0.24) and the corresponding membrane hydraulic permeability parameters listed in Table 2 for SMC, LNCaP and HDF, respectively [12,29,30]. This model, with the appropriate parameters taken from above and Table 2, is then used to predict volumetric behavior for a given cell type after seeding at −1 °C and equilibration prior to continuous cooling at 2 °C/min, thereby allowing comparison to volumetric data obtained from FTIR measurements.

2.3. FTIR setup and analysis

FTIR spectra were obtained using a Nicolet Magna 6700 spectrometer (Thermo-Nicolet, Madison, WI) equipped with a TGS detector. Spectra were acquired at 4 cm^{-1} resolution using 32 co-added interferograms between wavenumber ranges of 4000 and 900 cm^{-1} as previously reported [12,31]. The cell pellet samples were mounted onto a specialized temperature cell that was regulated using a temperature controller (Minco Products Inc., Minneapolis, MN). Sample

temperature, also monitored separately using a thermocouple, was decreased from room temperature to −80 °C at 2 °C/min. The phase change temperature of the cell media upon thawing is ~−0.6 °C, and depends only on its osmolality. However, the temperature of phase change during cooling depends on ice nucleation, which is a stochastic process that requires supercooling of the system. Hence all of the samples reported here are nucleated at temperatures well below the equilibrium phase change temperature (or melt) of the system. For example, for all IIF studies reported here ice nucleation occurred at or below −10 °C following supercooling of the system. For all dehydration studies, controlled ice nucleation was performed at −3 °C. Dehydration of cells is a consequence of the phase change of water to ice and not a precursor.

2.3.1. Membrane lipid analysis

Spectral analysis was carried out using Omnic software (Thermo-Nicolet, Madison, WI). Membrane phase behavior during freezing was monitored by observing the peak position of the νCH_2 symmetric stretching band at ~2850 cm^{-1} as described previously [31]. Ice formation induces phase transitions that cause a decrease in residual membrane conformational disorder in the frozen state. Dramatic changes in wavenumber for cells that have been cooled rapidly is closely associated with conformational disorder changes, and depends on the cooling rate and nucleation temperature. Wavenumber (νCH_2) versus temperature plots were constructed to capture freezing induced phase transitions (Fig. 1). The initial slope of νCH_2 versus temperature upon ice nucleation was taken as a measure for the dehydrating (lyotropic) effect of ice formation on membrane hydration. Arrhenius plots were constructed by plotting the natural logarithm of the initial rate of the membrane phase change upon ice formation versus the inverse of the nucleation temperature. The slope of the Arrhenius plots were then used to calculate the activation energy of the freezing induced membrane phase changes.

2.3.2. Water band analysis

The phase change of water into ice and vice versa was monitored by inspection of the H_2O bending and libration combination band between 2680 and 1950 cm^{-1} [32]. The area under the H_2O band (which includes water and ice) was calculated and plotted as a function of temperature. The intensity of this band increases upon ice formation due to the changes in hydrogen bonding interactions that occur as water changes phase. In addition to showing the onset of ice in the system, the H_2O band, monitored for the peak shift that occurs during the phase change of water, reveals differences between IIF and dehydrating freezing conditions. In order to directly compare the FTIR water band area data with cryomicroscopy data, the FTIR data were corrected and normalized. Since the effects of ice nucleation only occur after actual ice nucleation and propagation, all data were normalized to account for this. Briefly, the H_2O band area change is measured from directly prior to ice nucleation (i.e., at or near −3 °C for dehydration and −10 °C for IIF). All further increases in the H_2O band area for dehydration and IIF cases are then measured with respect to this origin. Furthermore, to separate lyotropic from thermotropic changes a linear regression line is obtained for the H_2O band area change from −30 °C to −80 °C, where no further biophysical changes are occurring in the IIF data set (NT = −10 °C). The line from this thermotropic effect is then extrapolated to higher temperatures and subtracted from both the dehydration and IIF data sets. Finally, both data sets are set to 0 at NT = −3 and NT = −10 °C, respectively.

2.3.3. Correlation of water band area to cellular biophysics

Excess water during freezing can be compared directly to the cellular biophysical response, as previously reported for DSC measurements [19–21]. To accomplish this for FTIR using H_2O band area changes, several steps are necessary. When ice is nucleated at −3 °C, the cells will reach equilibrium volume at this temperature, since there is a time lag between ice nucleation and FTIR spectral recording. This equilibrium cell volume (V_o) at −3 °C and the osmotically inactive cell volume (V_b) for the cell types in question are known, or can be calculated based on previous work [12,29,30]. This allows the corrected H_2O band area change to be converted to cellular volumetric change by using the following equation:

$$\frac{A(T)_{NT=-3\,^\circ C} - A(T)_{NT=-10\,^\circ C}}{A(-30\,^\circ C)_{NT=-3\,^\circ C} - A(-30\,^\circ C)_{NT=-10\,^\circ C}} = \frac{V_o - V(T)}{V_o - V_b}. \quad (3)$$

Here, A refers to the peak area under the H_2O band (see Fig. 5) at temperature T, and V refers to the corresponding predicted cellular volume that is in the range between V_o and V_b. The numerator of the LHS represents variable excess water at a given temperature during dehydration, while the denominator represents the total excess water at −30 °C (i.e., total excess water available from complete dehydration vs. IIF at −30 °C). By converting this to volumetric data (RHS) the data can be directly compared to previously established dehydration behavior for the same cell types or directly fit by Eqs. (1) and (2) by

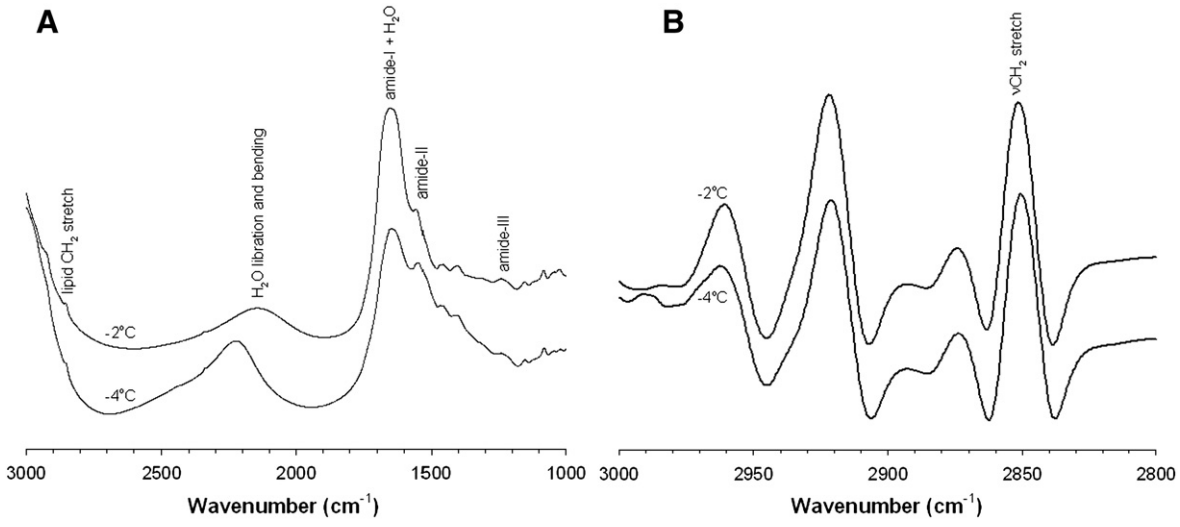

Fig. 1. In situ IR absorption spectra of HDF cells at −2 °C and −4 °C just before and after nucleation of the sample at −3 °C, respectively. Characteristic molecular group vibrations are indicated. (B) Second derivative profile of the spectra is included to highlight the characteristic –CH_2 vibrational bands associated with lipid acyl chains of the cells.

a non-linear regression algorithm to extract membrane hydraulic permeability parameters, as previously reported [12,29,30].

3. Results

FTIR is used to measure the phase state of the membrane and surrounding water during freezing of three mammalian cell types of widely differing size and biophysical properties: human dermal fibroblasts (HDF), porcine smooth muscle cells (SMC) and human LNCaP prostate tumor cells.

Fig. 1 depicts IR absorbance spectra of HDF cells at −2 °C and −4 °C (1 °C above and below, respectively, the ice nucleation temperature at −3 °C). The IR spectrum of the cells in media is dominated by the signal from water or from ice. Water exhibits strong vibrational bands at around 3300 cm^{-1}, 2200 cm^{-1}, and 1650 cm^{-1}, arising from stretching, libration and bending combination, and scissoring vibrational modes, respectively [12]. The frozen sample exhibits clear differences in spectral shape compared to the unfrozen cell samples. This is mostly due to shape changes of the water absorption bands upon transition into ice. The characteristic water band at 2200 cm^{-1} exhibits a clear change in its shape and position upon ice nucleation of the sample. The effect of ice formation on the H_2O band is further analyzed in Figs. 4 and 5. In the 3000–2800 cm^{-1} region, the symmetric and asymmetric –CH_2 stretching vibrations of lipid acyl chains are clearly visible on taking second derivative of the spectra (Fig. 1B). The lipid bands shift to lower wavenumber with decreasing temperature. This effect is further analyzed in Fig. 2 and below.

3.1. Membrane phase behavior during freezing

The effect of freezing on membrane conformational disorder was monitored by tracking the shift in the wavenumber position of the symmetric νCH_2 stretching band at ~2850 cm^{-1} with cooling for all cell types. Fig. 2 shows that nucleation at high subzero temperatures (dehydrating conditions at NT = −3 °C) coincides with a dramatic change in membrane conformational disorder in all cell types, which is not observed under IIF conditions (NT = −10 °C). Hence, the membrane phase behavior of SMC, HDF and LNCaP cells during freezing depends on the ice nucleation temperature. All cells display a highly cooperative membrane phase transition with nucleation at −3 °C, whereas ice nucleation at −10 °C causes a much less pronounced effect on the residual membrane conformational disorder in the frozen state. This implies that cell membranes tend to pack in a highly ordered gel phase under freezing conditions that cause cellular dehydration, whereas under freezing conditions that cause IIF, membranes remain relatively fluid (i.e. more conformational disorder) in the frozen state. Dehydrating conditions result in the removal of water from phospholipid head-groups and cause membranes to undergo a lyotropic liquid crystalline to gel phase transition.

The sharp decrease in νCH_2 following nucleation at −3 °C continues down to approximately −30 °C before leveling off to a constant slope. This initial effect of ice nucleation on membrane conformational disorder is cell specific. For example, the magnitude of change in νCH_2 is cell specific and is highest for HDFs (Fig. 2C) and lowest for SMCs (Fig. 2A). Note that SMCs exhibit a thermotropic phase transition upon cooling prior to ice formation, which is not observed in the other cells.

Cell specific events that occur in membranes during freezing are characterized by the initial slope of νCH_2 versus temperature from NT to ~ −30 °C (wavenumber temperature coefficient, WTC1), the wavenumber temperature coefficient from −30 °C to −80 °C (WTC2: the thermotropic change at lower temperatures) and the magnitude of the shift in wavenumber position from the ice nucleation temperature until −80 °C (ν_{shift}). Table 1 lists WTC1, WTC2, and ν_{shift} for the three cell types under dehydrating (NT = −3 °C) and IIF (NT = −10 °C) conditions. WTC1 and ν_{shift} are greatest for HDFs and smallest for SMCs whereas the thermotropic lipid response below −30 °C (WTC2), where cellular dehydration and IIF responses diminish or cease, is approximately the same irrespective of the cell type or the nucleation temperature. The change in the slope of νCH_2 at NT between −3 and −10 °C (WTC1) shows Arrhenius behavior for a representative cell type (LNCaP) as shown in Fig. 3. The activation energies that are thus determined for the three cell types are depicted in Table 2 and closely

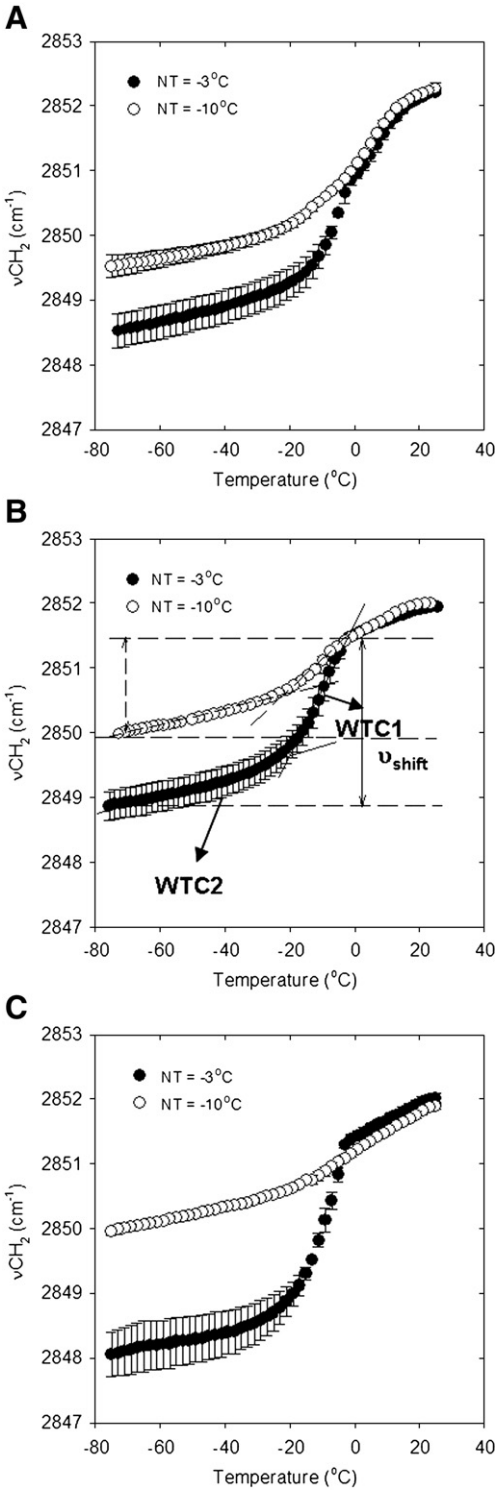

Fig. 2. Membrane phase behavior of (A) SMC, (B) LNCaP and (C) HDF cells during cooling and nucleation at −3 °C (filled circles) and −10 °C (open circles). The data points reflect the wavenumber position of the symmetric –CH_2 stretching vibration (νCH2) arising from the lipid acyl chains with corresponding standard error ($n = 3$).

Table 1
Characteristic cell specific parameters extracted from the membrane phase behavior of SMC, LNCaP and HDF cells following spectral analysis of the FTIR freezing data.

Cell type	Dehydrating conditions (ice formation at −3 °C)			IIF conditions (ice formation at −10 °C)		
	WTC1 (cm^{-1}/°C)	WTC2 (cm^{-1}/°C)	ν_{shift} (cm^{-1})	WTC1 (cm^{-1}/°C)	WTC2 (cm^{-1}/°C)	ν_{shift} (cm^{-1})
SMC	0.105 ± 0.012	0.017 ± 0.002	2.13 ± 0.74	0.080 ± 0.015	0.015 ± 0.004	1.34 ± 0.25
LNCaP	0.13 ± 0.03	0.02 ± 0.003	2.61 ± 0.34	0.058 ± 0.003	0.02 ± 0.002	1.43 ± 0.07
HDF	0.221 ± 0.005	0.017 ± 0.008	3.24 ± 0.53	0.039 ± 0.004	0.013 ± 0.001	1.13 ± 0.16

WTC1 reflects the initial wavenumber temperature coefficient at the onset of ice nucleation, WTC2 refers to the wavenumber versus temperature coefficient below −30 °C and ν_{shift} is the wavenumber shift from the nucleation temperature to −80 °C. ν_{shift} refers to the shift in wavenumber position from the ice nucleation temperature until −80 °C.

match the activation energies for water transport (E_{Lp}) as determined by cryomicroscopy.

3.2. Cellular associated water/ice

The extreme loss of lipid hydration in the membrane under dehydrating freezing conditions is expected to result in a greater amount of ice formed in the sample during dehydration, when compared to IIF conditions. The formation of both intracellular and extracellular ice under dehydrating and IIF conditions was studied here by inspection of the libration and bending combination band of H_2O (Fig. 4).

Panels A and B of Fig. 4 show 3D spectral plots of the H_2O bands during freezing of LNCaP cell pellets for NT = −3 °C (dehydrating conditions) and NT ~ −10 °C (IIF conditions), respectively. On ice formation, the spectral peak shifts to a higher wavenumber position while the width of the spectra narrows and the associated band area increases, denoting a change in the hydrogen bonding interactions. Fig. 4A shows that ice nucleation at high subzero temperatures (−3 °C) results in a gradual increase in the H_2O band area before leveling off at −30 °C. By contrast, at NT ~ −10 °C, there is minimal increase in the H_2O band area upon further temperature drop.

In Fig. 5, the total increase in the H_2O band area from room temperature until −80 °C is plotted. For all cell types, there is an increase in the total amount of water changing phase under dehydrating conditions as compared to IIF nucleating conditions. The magnitude of the increase in the excess ice formed is cell type dependent and is highest for HDFs and least for SMCs. Under IIF conditions (NT ~ −10 °C), a relatively small monotonous increase in H_2O band area is observed with decreasing temperature, irrespective of cell type. This increase is not due to ice formation but due to changes in hydrogen bonding interactions upon cooling (thermotropic effect). This thermotropic change in H_2O band area is also observed below −30 °C under dehydrating conditions (slopes are similar below −30 °C). Thus, the thermotropic effect is subtracted from the overall data for comparison with the cellular dehydration data predicted from cryomicroscopy measurements, according to Eq. (3) as described in the Materials and methods section (Fig. 6). For comparison, the solid lines in Fig. 6 are comparisons of cellular volumetric changes for each cell type at 2 °C/min, predicted from previously published cryomicroscopy studies [11,28,29]. The slight lag of the FTIR data at temperatures from −4 to −10 °C is likely due to differences in experimental set-up (see Materials and methods and Discussion).

Fig. 7 shows that the increased ice formation under dehydrating conditions coincides with strong membrane dehydration, suggesting that the extra ice in the system comes from bound or membrane associated water around lipids (and other biomolecules). A comparison of the first derivatives (Fig. 7B) demonstrates that the maximum of H_2O band area change during freezing closely coincides with the maximum of the membrane phase change. This suggests that the membrane phase change is lyotropic and is a consequence of membrane dehydration.

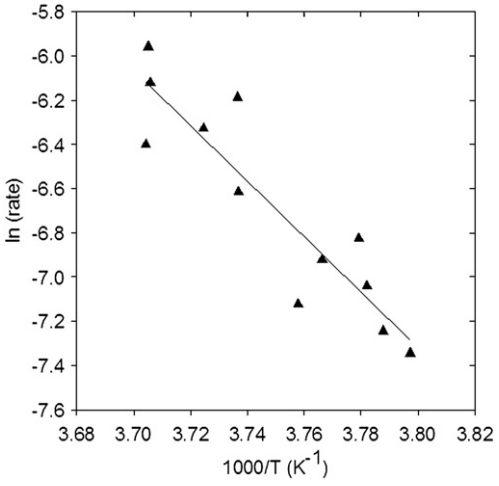

Fig. 3. Arrhenius plot of the initial rate of the membrane phase change upon ice nucleation and the ice nucleation temperature for LNCaP cells. Data obtained from Wolkers et al. [12] were used to construct the plot.

4. Discussion

We recently reported that the state of membrane lipids during freezing correlates with cellular biophysics (i.e., dehydration and IIF) and viability post-freezing of human LNCaP prostate tumor cells [12]. Here we show the generality of this result in a variety of mammalian cells of varying size and biophysical properties (i.e., porcine smooth muscle cells (SMC) and human dermal fibroblasts (HDF)). In addition, we show that lipid hydration is a likely source of excess H_2O during phase change and is the mechanism for reduction in water transport at subzero temperatures. Finally, the drastic change in lipid hydration during cellular dehydration suggests a possible link to freeze-induced "solution effects" injury mechanism(s) [1].

4.1. Cellular biophysics

Unlike cryomicroscopy and DSC techniques that allow faster cooling rates, the current FTIR method can only vary nucleation temperature while the cooling rate is limited to 2 °C/min or less. Thus,

Table 2
The membrane hydraulic permeability (L_{pg}) and the activation energy for water transport (E_{Lp}) as determined from FTIR data compared to previously determined cryomicroscopy data on these parameters.

Cell type	Cell permeability L_{pg} (μm/min atm)		Activation energy E_{Lp} (kcal/mol)	
	Cryomicroscope (model prediction)	FTIR	Cryomicroscope (model prediction)	FTIR
SMC	0.12	0.07	24.1	22.5
LNCaP	0.21	0.24	25.1	25.0
HDF	0.10	0.08	42.0	41.0

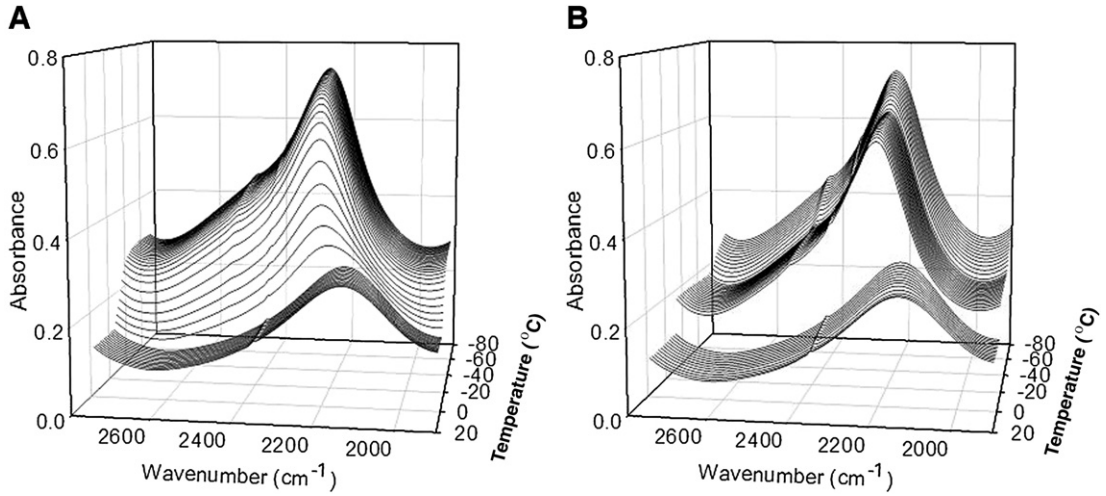

Fig. 4. Contour plot of the H_2O spectral band during cooling of LNCaP cell pellets from room temperature to −80 °C at 2 °C/min with ice nucleation at (A) −3 °C and (B) −10 °C. The phase change of water into ice during freezing manifests itself as a narrowing of the H_2O spectral band with a corresponding shift of the peak to higher wavenumbers and an increase in band intensity.

varying the ice nucleation temperature in the FTIR method determines the cellular biophysical outcome (i.e., cellular dehydration or IIF) while cooling rate is fixed at 2 °C/min. For ice nucleation at −3 °C and the subsequent temperature decrease, the cells are subjected to increasing solute concentrations that lead to cellular dehydration. However, this is not the case when ice nucleation occurs at −10 °C, where the bulk of the supercooled water is trapped inside the cells resulting in IIF. Excess available H_2O resulting from cell dehydration, presumably from dehydration of macromolecular structures including the membrane (i.e., reduction in hydration and head group area for lipids) is expected to increase the total amount of extracellular ice for NT = −3 °C vs. −10 °C or below. This increased water content under dehydrating conditions is captured in the increase in the H_2O band area during cooling (Fig. 4). Dehydration also coincides with a phase transition and its associated conformational change of the membranes (Fig. 7). Specifically, a strong freezing induced lyotropic phase transition is observed during dehydrating conditions (NT = −3 °C), indicating removal of bound water, predominantly around the lipid head groups, that is otherwise unfrozen and unavailable for phase change during IIF conditions (NT = −10 °C).

Excess H_2O band area is linked to cellular biophysics by the proposal that this water is derived from the membrane during cellular dehydration and is proportional to the normalized cell volume. This hypothesis is supported by DSC studies which show that excess heat is released from intact cells and tissues during freezing induced dehydration, but not during IIF or cell lyses, and that this heat release correlates strongly to normalized cellular volume in the sample [19–21]. Applying this hypothesis to the FTIR data, the excess ice peak can be correlated to cellular dehydration as shown in Eq. (3). These data are then compared directly to correlative cellular data obtained by cryomicroscopy, as shown in Fig. 6.

Cellular dehydration predicted by FTIR matches reasonably well with the cryomicroscopy data (Fig. 6). It should be noted that the starting cell volumes are different and there is a slight lag in FTIR data vs. the cryomicroscopy data in the intermediate subzero temperature range (approximately −4 to −10 °C). The starting cell volume difference can be explained by the fact that cryomicroscopy typically starts after seeding and equilibration at −1 °C, whereas FTIR is seeded at −3 °C and below during continuous cooling. The lag below −4 °C is attributed to cryomicroscopy being carried out on a cell suspension while FTIR is carried out on a cell pellet, where cell density is expected to reduce dehydration kinetics, as previously reported [16]. With these caveats in mind, FTIR can be used to measure and predict cellular biophysics, provided the initial and non-solvent volumes of the given cell are known (V_o and V_b, respectively, in Eq. (3)). Interestingly, the membrane phase change and corresponding lipid hydration during cell freezing yield cell specific activation energies (Table 2) that match closely the activation energy of water transport (E_{Lp}) as predicted by cryomicroscopy. This strongly suggests that a reduction in the lipid hydration or head group area is in fact the mechanism whereby the water transport is reduced at subzero temperatures. This reduction in the hydraulic permeability with temperature is captured in the activation energy (Eq. (2)).

4.2. Correlation to injury

Ice nucleation temperature has a profound effect on the membrane lipid phase behavior of the cells. It has been established that removal of water predominantly from the phospholipid head groups causes lyotropic phase transitions during air-drying [33]. Freezing also has a similar dehydrating effect on liposomal systems [11]. Here, we show that freezing can also cause such lyotropic phase changes in a variety of mammalian cells during freezing. The magnitude of freezing induced lyotropic membrane phase changes decreases with the extent of supercooling. During supercooling more water will be trapped inside the cells, which increases the incidence of IIF. For all cell types studied, the onset of the liquid crystalline to gel phase transition coincided with the ice nucleation temperature. Freezing induced water transport and membrane phase changes have been shown to be closely associated events. The membrane phase behavior during freezing is a cell specific response, and must be associated with the cell's lipid composition and cholesterol content. In the case of the SMC, a thermotropic phase transition is evident prior to ice formation in the sample. However, the lyotropic phase transition upon ice nucleation is still greater than the thermotropic phase transition. Steponkus suggested that freezing induced lamellar to hexagonal phase transition is responsible for cell death during freeze/thaw of plant protoplasts, using freeze fracture analysis [3,6]. Our results in mammalian cells do not indicate the formation of hexagonal phase during freezing but point to a tight gel phase where lipid hydration is reduced. It has been established that for lipid bilayers in liposomal systems, maximal leakage of intra-liposomal contents coincides closely with the phase transition temperature [34]. Hence, it is possible that freezing induced dehydration damage occurs as a result of leakage of cytoplasmic compounds during the phase transition, either during cooling or thawing. Nucleation at high subzero temperatures

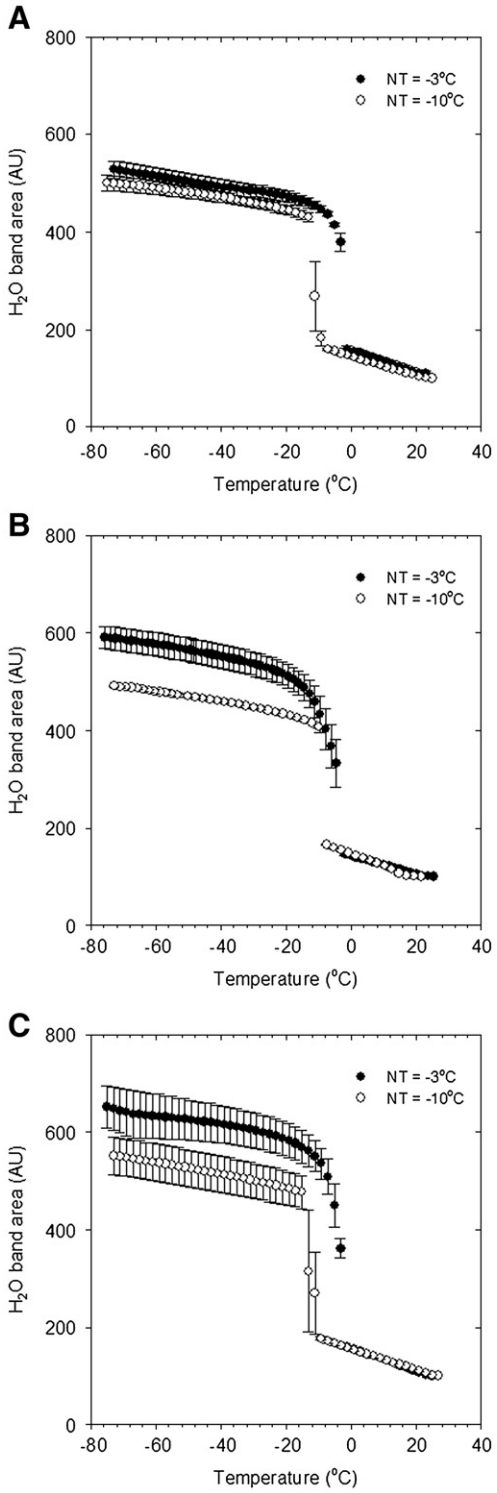

Fig. 5. H_2O (water or ice) spectral band area versus temperature plots from room temperature to −80 °C for (A) SMC, (B) LNCaP and (C) HDF cells with ice nucleation temperatures of −3 °C (filled circles) and −10 °C (open circles) with corresponding standard error ($n=3$). In all cases, the total amount of ice that is formed under dehydrating freezing conditions (NT = −3 °C) is greater than that under IIF conditions (NT = −10 °C).

followed by slow cooling, which is known to cause "solution effects" injury [1], is shown here to cause membranes to become severely dehydrated. The data suggest that "solution effects" injury is associated with a dramatic loss of membrane-associated water around the phospholipid head groups.

In addition to quantifying the state of water and membrane lipid phase changes in cells during freezing, FTIR can be used to simultaneously probe possible mechanisms of cellular injury. Fig. 8 depicts the normalized lipid wavenumber (membrane phase state) of LNCaP cells under different nucleation temperatures against observed cell viability. An inverted U shape dependence (dotted line represents a typical cryobiological viability outcome) is predicted from experi-

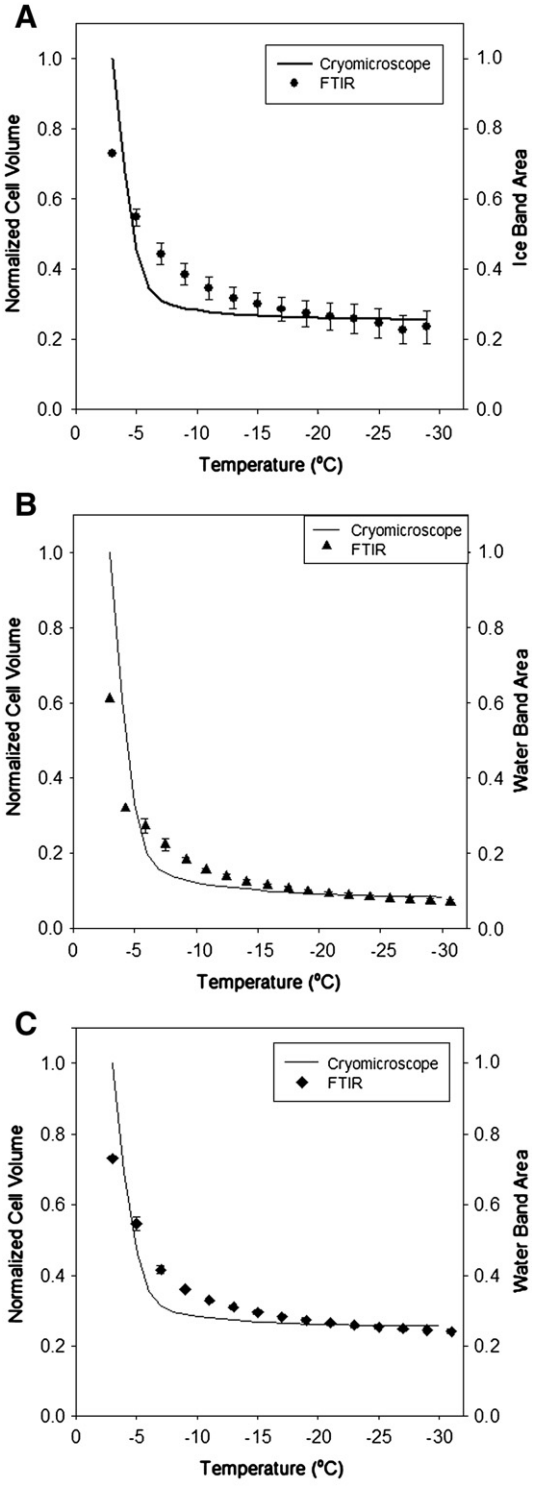

Fig. 6. Comparison of the cellular volumetric changes as a result of freeze induced dehydration as predicted from FTIR spectral H_2O band area with cellular volume predicted from cryomicroscopy measurements [12,29,30] for (A) SMC, (B) LNCaP and (C) HDF cells.

mental data [12]. Minimal survival is obtained at the extremes (i.e., NT = −3 and −10 °C) as a consequence of "solution effects" injury and IIF, respectively, that are linked here to residual membrane conformational disorder in the frozen state. The LNCaP membrane lipid wavenumber at −30 °C increases from its lowest during dehydration (2849.4 cm^{-1} at NT = −3 °C) to its highest during IIF (2850.5 cm^{-1} at NT = −10 °C). At an intermediate NT (−6 °C), the lipid wavenumber observed is between those for the dehydrated and the IIF conditions (2849.7 cm^{-1}). This is a consequence of a reduction in cellular dehydration, which allows a certain amount of cellular (and membrane) bound water to remain in the cell. It is at this intermediate condition (for both NT and residual membrane conformational disorder) that cell viability is highest [12].

The nucleation temperature yielding optimal survival coincides with intermediate residual membrane conformational disorder levels in the frozen state that occurs between dehydrating and IIF conditions. At room temperature, equilibrium exists between the hydration forces and the compressive stress of the lipid lamellae that maintains the rigidity of the lipid structure. However, as the cell dehydrates, the lipid membrane experiences an increase in both the lateral compressive and hydration stresses (i.e., a decrease in head group hydration). The increased lateral compressive stresses cause a transition in the lipid membrane from a liquid lamellar to a gel phase [4]. When cell dehydration becomes more severe, loss of lipid hydration and head group area correlates with increased cell death (Fig. 8). This will lead to a continual decrease in the distance between lipid head groups and lipid lamellae as compared to its initial liquid state.

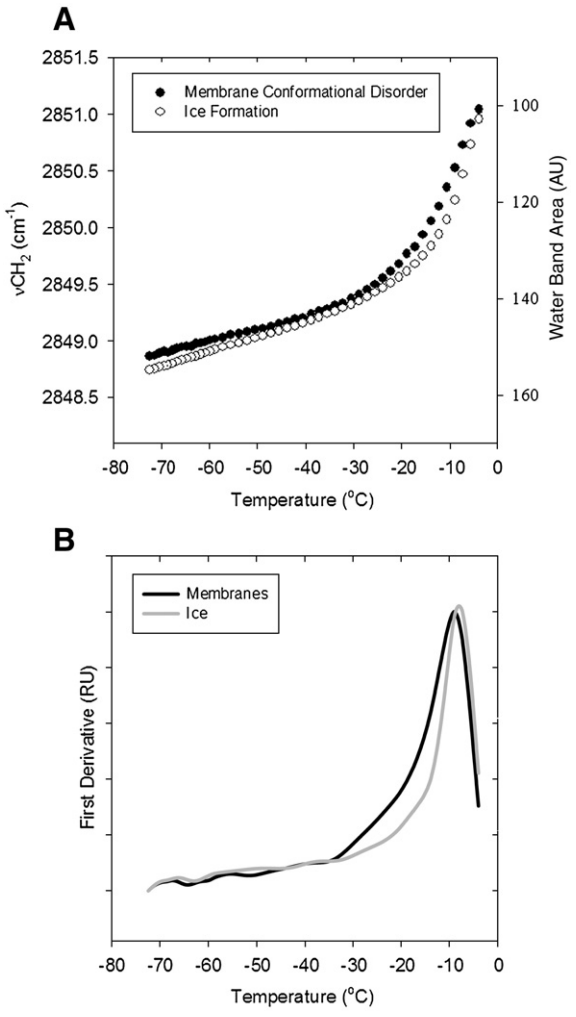

Fig. 7. (A) Cell membrane conformational disorder changes in LNCaP cells concomitantly with dehydration during freezing from −3 °C to −80 °C. (B) First derivative of the changes in membrane conformational disorder and the H_2O band area with temperature decrease for LNCaP cells.

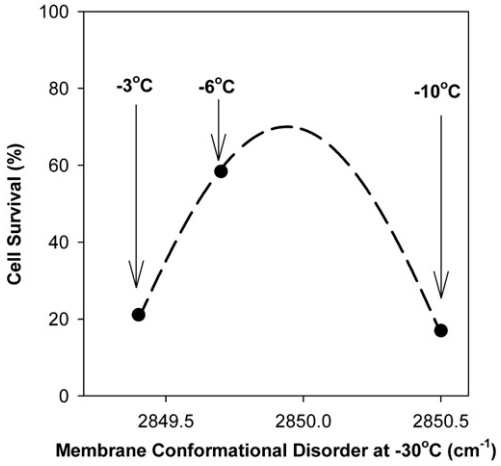

Fig. 8. Membrane conformational disorder changes of LNCaP cells at −30 °C under different ice nucleation temperatures vs. experimentally determined cell viability after freezing and thawing. The dotted line represents an inverted U shaped fit (generally associated with cellular viability under different nucleating conditions) to the representative points. Cell viability data on freeze survival obtained from Wolkers et al. [12] were used to construct the plot.

Reduction in head group area or hydration layers of the lipids below some critical value is therefore suggested by our studies as a possible cause of cell injury for the −3 °C NT cooling cases. These conditions expose the cell, and the biomolecules of the cell (including the membrane), to conditions of minimal supercooling, slow cooling and higher solute concentrations than during more rapid cooling where supercooling prevents high solution exposure. This is believed to be at the heart of the "solution effects" mechanism of injury in cryobiology [1,35]. The current data are among the first to show the connection between cellular and membrane dehydration. We propose that this connection is also linked to a molecular mechanism of injury for the "solution effects" injury that would suggest that membranes tolerate dehydration only to a certain extent. For instance, at −6 °C, the loss of lipid hydration is not as extreme as for −3 °C NT and is more favorable for cell survival. This state is indeed intermediate between the most hydrated, IIF conditions (NT < −10 °C) and the least hydrated conditions (NT = −3 °C). Under IIF conditions, ice formation appears to have little effect on the membrane, leaving lipids relatively hydrated and in high conformational disorder.

Acknowledgements

The authors would like to acknowledge grant support from National Institute of Health (NIH) R01-CA07528. The authors would also like to thank Dr. Alptekin Aksan for valuable discussions, Dr. Joel Slaton and the MD Anderson Cancer Center for the LNCaP Pro5 line cells.

References

[1] P. Mazur, S.P. Leibo, E.H. Chu, A two-factor hypothesis of freezing injury. Evidence from Chinese hamster tissue-culture cells, Exp. Cell Res. 71 (1972) 345–355.
[2] H.L. Casal, H.H. Mantsch, Polymorphic phase behavior of phospholipid membranes studied by infrared spectroscopy, Biochim. Biophys. Acta 779 (1984) 381–401.
[3] P.L. Steponkus, D.V. Lynch, Freeze/thaw-induced destabilization of the plasma membrane and the effects of cold acclimation, J. Bioenerg. Biomembranes 21 (1989) 21–41.

[4] J. Wolfe, G. Bryant, Freezing, drying and/or vitrification of membrane–solute–water systems, Cryobiology 39 (1999) 103–139.
[5] W.J. Gordon Kamm, P.L. Steponkus, Lamellar-to-hexagonalII phase transitions in the plasma membrane of isolated protoplasts after freeze-induced dehydration, Proc. Natl. Acad. Sci. 81 (1984) 6373–6377.
[6] P.L. Steponkus, M. Uemura, R.A. Balsamo, T. Arvinte, D.V. Lynch, Transformation of the cryobehavior of rye protoplasts by modification of the plasma membrane lipid composition, Proc. Natl. Acad. Sci. 85 (1988) 9026–9030.
[7] J.E. Lovelock, The mechanism of the protective action of glycerol against haemolysis by freezing and thawing, Biochim. Biophys. Acta 11 (1953) 28–36.
[8] J. Wolfe, M.F. Dowgert, P.L. Steponkus, Mechanical study of the deformation and rupture of the plasma membranes of protoplasts during osmotic expansions, J. Membr. Biol. 93 (1986) 63–74.
[9] H.T. Meryman, Freezing injury and its prevention in living cells, Annu. Rev. Biophys. Bioeng. 3 (1974) 341–363.
[10] D. Chapman, The role of water in biomembrane structures, J. Food Eng. 22 (1994) 367–380.
[11] M. Caffrey, The combined and separate effects of low temperature and freezing on membrane lipid mesomorphic phase behavior: relevance to cryobiology, Biochim. Biophys. Acta 896 (1987) 123–127.
[12] W.F. Wolkers, S.K. Balasubramanian, E.L. Ongstad, H.C. Zec, J.C. Bischof, Effects of freezing on membranes and proteins in LNCaP prostate tumor cells, Biochim. Biophys. Acta 1768 (2007) 728–736.
[13] J.F. Brouwers, B.M. Gadella, In situ detection and localization of lipid peroxidation in individual bovine sperm cells, Free Radic. Biol. Med. 35 (2003) 1382–1391.
[14] K.R. Diller, Quantitative low temperature optical microscopy of biological systems, J. Microsc. 126 (1982) 9–28.
[15] K.R. Diller, E.G. Cravalho, A cryomicroscope for the study of freezing and thawing processes in biological cells, Cryobiology 7 (1970) 191–199.
[16] R.L. Levin, E.G. Cravalho, C.E. Huggins, A membrane model describing the effect of temperature on the water conductivity of erythrocyte membranes at subzero temperatures, Cryobiology 13 (1976) 415–429.
[17] P. Mazur, Kinetics of water loss from cells at subzero temperatures and the likelihood of intracellular freezing, J. Gen. Physiol. 47 (1963) 347–369.
[18] M. Toner, E.G. Cravalho, M. Karel, Thermodynamics and kinetics of intracellular ice formation during freezing of biological cells, J. Appl. Physi. 67 (1990) 1582–1593.
[19] R.V. Devireddy, J.C. Bischof, Measurement of water transport during freezing in mammalian liver tissue: Part II — the use of differential scanning calorimetry, J. Biomech. Eng. 120 (1998) 559–569.
[20] R.V. Devireddy, D. Raha, J.C. Bischof, Measurement of water transport during freezing in cell suspensions using a differential scanning calorimeter, Cryobiology 36 (1998) 124–155.
[21] R.V. Devireddy, D.J. Swanlund, K.P. Roberts, J.C. Bischof, Subzero water permeability parameters of mouse spermatozoa in the presence of extracellular ice and cryoprotective agents, Biol. Reprod. 61 (1999) 764–775.
[22] J.H. Crowe, F.A. Hoekstra, L.M. Crowe, T.J. Anchordoguy, E. Drobnis, Lipid phase transitions measured in intact cells with Fourier transform infrared spectroscopy, Cryobiology 26 (1989) 76–84.
[23] D.G. Cameron, A. Martin, H.H. Mantsch, Membrane isolation alters the gel to liquid crystal transition of *Acholeplasma laidlawii B*, Science 219 (1983) 180–182.
[24] J.H. Crowe, L.M. Crowe, D. Chapman, Preservation of membranes in anhydrobiotic organisms: the role of trehalose, Science 223 (1984) 701–703.
[25] H. Hao, P. Ropraz, V. verin, E. Camenzind, A. Geinoz, M.S. Pepper, G. Gabbiani, M.L. Bochaton-Piallat, Heterogenity of smooth muscle cell populations cultured from pig coronary artery, Arterioscler. Thromb. Vasc. Biol. 22 (2002) 1093–1099.
[26] E.D. Grassl, J.C. Bischof, In vitro model systems for evaluation of smooth muscle cell response to cryoplasty, Cryobiology 50 (2005) 162–173.
[27] J.J. McGrath, Membrane Transport Properties, ASME, New York, 1988.
[28] R.E. Pitt, Cryobiological implications of different methods of calculating the chemical potential of water in partially frozen suspending media, Cryoletters 11 (1990) 227–240.
[29] S.K. Balasubramanian, J.C. Bischof, A. Hubel, Water transport and IIF parameters for a connective tissue equivalent, Cryobiology 52 (2006) 62–73.
[30] S.K. Balasubramanian, R.T. Venkatasubramanian, A. Menon, J.C. Bischof, Thermal injury prediction during cryoplasty through in vitro characterization of smooth muscle cell biophysics and viability, Ann. Biomed. Eng. 36 (2008) 86–101.
[31] W.F. Wolkers, L.M. Crowe, N.M. Tsvetkova, F. Tablin, J.H. Crowe, In situ assessment of erythrocyte membrane properties during cold storage, Mol. Membr. Biol. 19 (2002) 59–65.
[32] S.Y. Venyaminov, F.G. Prendergast, Water (H_2O and D_2O) molar absorptivity in the 1000–4000 cm^{-1} range and quantitative infrared spectroscopy of aqueous solutions, Anal. Biochem. 248 (1997) 234–245.
[33] J.H. Crowe, A.E. Oliver, F.A. Hoekstra, L.M. Crowe, Stabilization of dry membranes by mixtures of hydroxyethyl starch and glucose: the role of vitrification, Cryobiology 35 (1997) 20–30.
[34] L.M. Hays, J.H. Crowe, W.F. Wolkers, S. Rudenko, Factors affecting leakage of trapped solutes from phospholipid vesicles during thermotropic phase transitions, Cryobiology 42 (2001) 88–102.
[35] P. Mazur, Freezing of living cells: mechanisms and implications, Am. J. Physiol. 143 (1984) C125–C142.